Synthesis and Properties of 5-Chloro-8-hydroxyquinoline-Substituted Azacrown Ethers: A New Family of Highly Metal Ion-Selective Lariat Ethers

Andrei V. Bordunov, Jerald S. Bradshaw,* Xian Xin Zhang, N. Kent Dalley, Xiaolan Kou, and Reed M. Izatt*

Department of Chemistry and Biochemistry, Brigham Young University, Provo, Utah 84602-5700

Received August 22, 1996[⊗]

New 5-chloro-8-hydroxyquinoline (CHQ)-substituted aza-18-crown-6 (**4**), diaza-18-crown-6 (**1**), diaza-21-crown-7 (**2**), and diaza-24-crown-8 (**3**) ligands, where CHQ was attached through the 7-position, and aza-18-crown-6 (**11**) and diaza-18-crown-6 (**10**) macrocycles, where CHQ was attached through the 2-position, were prepared. Thermodynamic quantities for complexation of these CHQ-substituted macrocycles with alkali, alkaline earth, and transition metal ions were determined in absolute methanol at 25.0 °C by calorimetric titration. Two isomers, **1** and **10**, which are different only in the attachment positions of the CHQ to the parent macroring, exhibit remarkable differences in their affinities toward the metal ions. Compound **1** forms very stable complexes with Mg^{2+}, Ca^{2+}, Cu^{2+}, and Ni^{2+} (log K = 6.82, 5.31, 10.1, and 11.4, respectively), but not with the alkali metal ions. Ligand **10** displays strong complexation with K^+ and Ba^{2+} (log K = 6.61 and 12.2, respectively) but not with Mg^{2+} or Cu^{2+}. The new macrocycles and their complexes have been characterized by means of UV−visible and ^{1}H NMR spectra and X-ray crystallography. New peaks in the UV spectrum of the Mg^{2+}−**1** complex could allow an analytical determination of Mg^{2+} in very dilute solutions in the presence of other alkali and alkaline earth metal cations. ^{1}H NMR spectral and X-ray crystallographic studies indicate that ligand **10** forms a cryptate-like structure when coordinated with K^+ and Ba^{2+}, which induces an efficient overlap of the two hydroxyquinoline rings. Such overlapping forms a pseudo second macroring that results in a significant increase in both complex stability and cation selectivity.

Introduction

The metal ion complexing abilities of crown ethers can be improved significantly by functionalizing them with ligating side arms. Attachment of donating groups can also improve cation selectivity and transport through liquid membranes.[1] UV active or fluorophoric side arms on lariat ethers allow an analytical determination of certain cations by spectrophotometric methods because of the selectivity of cation binding and the specific UV or fluorecence response of the complexed material.[2]

The synthesis of azacrown ethers containing phenolic side arms has been reported.[3] A strong affinity for Ca^{2+}, Sr^{2+}, Ba^{2+}, K^+, Li^+, and Pb^{2+} was found for the mono- and diazacrown ethers containing phenolic groups.[2b−j] These macrocycles are also effective chromogenic reagents for the extraction of those cations from water into an organic phase. Phenol-containing lariat ethers can form covalent complexes as well as complexes with ion-pair binding between the phenoxide oxygen and metal cation. The strength of this interaction depends on cation surface-charge density.[2j] Moreover, selective coordination of particular cations by certain phenol-containing crown ethers can be realized by variation of other parameters such as the pH of the media; acidity of the phenolic OH groups; dimensions of the macrocyclic ring; type, number, and position of complexing heteroatoms; and the stereochemistry imposed by the arms which connect the phenolic groups to the macrocycle. There are many open-chain analytical reagents that contain phenolic units such as 8-hydroxyquinoline, 1-(2-pyridylazo)-2-naphthol, 4-(2-pyridylazo)resorcinol, 2-(5-bromo-2-pyridylazo)-5-(diethylamino)phenol, and 1-nitroso-2-naphthol.[4a] The cooperative interaction of OH groups of those reagents and their soft donating centers with metal cations allow strong binding with a wide range of cations. Most of these reagents are not selective. We expected that combining them with crown fragments would considerably improve cation recognition because of the steric requirements of the crown macrocycle.

There are at least four other advantages of such ligands: (1) In spite of the solubility of uncharged coordination-saturated complexes of analytical reagents in organic solvents, there are many examples where charged and/or coordination-unsaturated chelates can be extracted into organic solvents only when additional auxiliary ligating groups are present.[4a] Modification of analytical reagents with crown-ethers should improve the solubility of the complexes and allow their extraction into an organic phase because the donating centers of the crown ethers

[⊗] Abstract published in *Advance ACS Abstracts,* November 15, 1996.

(1) (a) Gatto, V. J.; Gokel, G. W. *J. Am. Chem. Soc.* **1984**, *106*, 8240. (b) Gatto, V. J.; Arnold, K. A.; Viscariello, A. M.; Miller, S. R.; Morgan, C. R.; Gokel, G. W. *J. Org. Chem.* **1986**, *51*, 5373. (c) Tsukube, H.; Yamashita, K.; Iwachido, T.; Zenki, M. *Tetrahedron Lett.* **1989**, *30*, 3983. (d) Tsukube, H.; Adachi, H.; Morosawa, S. *J. Chem. Soc., Perkin Trans. 1* **1989**, 89. (e) Matsumoto, K.; Minatogawa, H.; Munakata, M.; Toda, M.; Tsukube, H. *Tetrahedron Lett.* **1990**, *31*, 3923.

(2) (a) Shinkai, S.; Ishikawa, Z.; Shinkai, H.; Tsuno, T.; Makishima, H.; Ueda, K.; Manabe, O. *J. Am. Chem. Soc.* **1984**, *106*, 1801. (b) Nishida, H.; Katayama, Y.; Katsuki, H.; Nakamura, H.; Takagi, M.; Ueno, K.; *Chem. Lett.* **1982**, 1853. (c) Sakai, Y.; Kawano, N.; Nakamura, H.; Takagi, M. *Talanta* **1986**, *33*, 407. (d) Katayama, Y.; Fukuda, R.; Iwasaki, T.; Nita, K.; Takagi, M. *Anal. Chim. Acta* **1988**, *204*, 113. (e) Nakamura H.; Sakka, H.; Takagi, M.; Ueno, K. *Chem. Lett.* **1981**, 1305. (f) Nakamura H.; Nita, K.; Takagi, M.; Ueno, K. *Heterocycles* **1984**, *21*, 762. (g) Nishida, H.; Tazaki, M.; Takagi, M.; Ueno, K. *Mikrochim. Acta* **1981**, *1*, 281. (h) Shiga, M.; Nishida, H.; Nakamura, M.; Takagi, M.; Ueno, K. *Bunseki Kagaku* **1983**, *32*, E293. (i) Katayama, Y.; Fukuda, R.; Takagi, M. *Anal. Chim. Acta* **1986**, *185*, 295. (j) Katayama, Y.; Nita, K.; Ueda, M.; Nakamura, H.; Takagi, M. *Anal. Chim Acta* **1985**, *173*, 193.

(3) For a review, see: McDaniel, C. W.; Bradshaw, J. S.; Izatt, R. M. *Heterocycles* **1990**, *30*, 665.

(4) (a) Ueno, K.; Imamura, T.; Cheng, K. L. *Handbook of Organic Analytical Reagents,* 2nd ed.; CRC Press, Inc.: Boca Raton, FL, 1992. (b) Van Veggel, F. C. J. M.; Verboom, W.; Reinhoudt, D. N. *Chem. Rev.* **1994**, *94*, 279.

S0020-1669(96)01029-4 CCC: $12.00

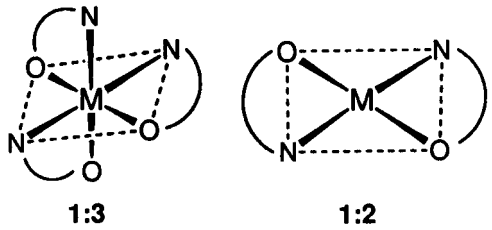

Figure 1. 8-Hydroxyquinoline chelate complexes.

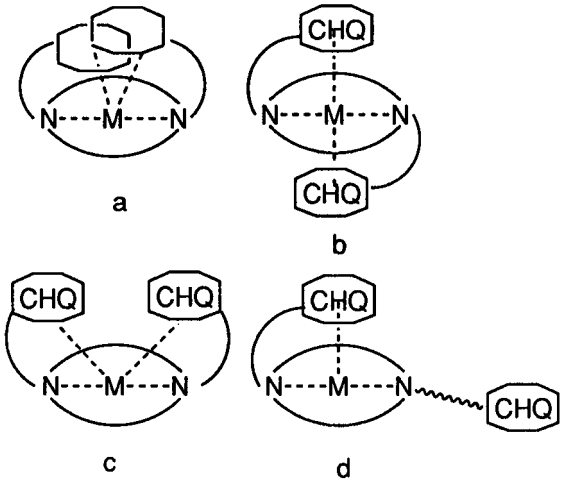

Figure 2. Coordination of the cation in *N*,*N*′-bis(5-chloro-8-hydroxyquinoline)diaza-18-crown-6 complexes.

can play the role of an auxiliary ligating group. This should allow transport of the complexed cations through liquid membranes. (2) Complexes of most known aromatic and heteroaromatic analytical reagents are insoluble in water. Attaching these reagents as side arms to the hydrophilic crown ethers should increase solubility of the complexes in water and allow the concentration of the cations to be determined without extraction. (3) Most of the mentioned reagents are UV and/or fluorescence active ligands. Thus, the functionalized crown ethers could be used as indicators of the complexed cation. (4) Crown ethers with attached chelate complexing sites are appropriate receptors for simultaneous binding of alkaline earth and transition metal cations.[4b]

8-Hydroxyquinoline has been used extensively as an extraction, chromogenic, and precipitation reagent in analysis.[5] Most 8-hydroxyquinoline chelate complexes have a 1:3 or 1:2 ratio of cation to ligand (Figure 1, only coordination-saturated uncharged chelates are shown). We have a special interest in the synthesis of 8-hydroxyquinoline-containing diazacrown ethers because of the possibility for 1:2 coordination of cations with two 8-hydroxyquinoline moieties in one molecule (Figure 2). Such functionalized diazacrown ethers may have three advantages. First, formation of a stable chelate ring between 8-hydroxyquinoline and a metal ion should stabilize the complex of the metal ion with the macrocyclic ligand. Second, the 8-hydroxyquinoline-functionalized crown ethers should improve cation selectivity. Attachment of two rigid 8-hydroxyquinoline groups to the diazacrown ring results in an appropriate preorganization of the ligand. Only the cation(s) whose size fits

Scheme 1. Preparation of 5-Chloro-8-hydroxy-7-quinolinyl- and 4-Chlorophenol-Substituted Azacrown Ether Ligands **1**−**4** and **9**

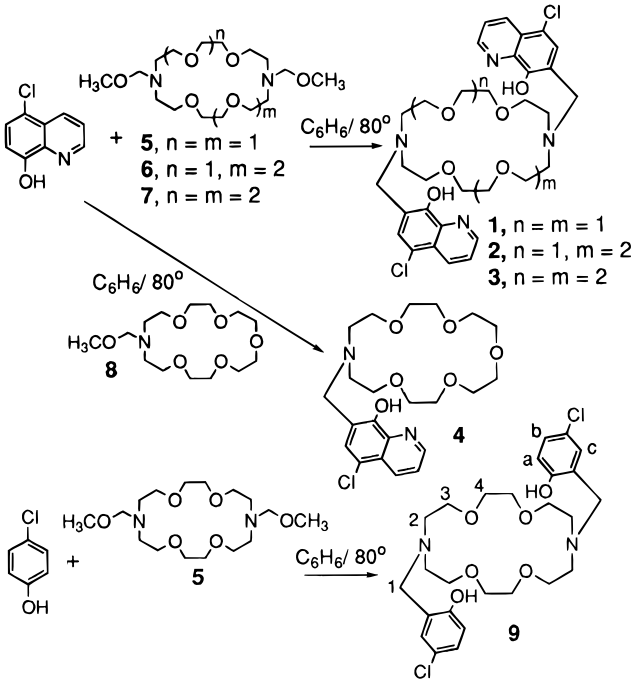

the pseudo-three-dimensional cavity of the macrocycle may bring every donor site to a position where they can interact with the cation(s) without causing a large macroring deformation. Finally, it is possible for the two 8-hydroxyquinoline moieties of the macrocyclic ligand to overlap each other through an intramolecular interaction so that a cryptate-like structure could be formed.[6] This effect brings a further increase in complex stability and cation selectivity.

In this paper we report the synthesis and properties of eight new 5-chloro-8-hydroxyquinoline-substituted azacrown ethers. Thermodynamic, UV−visible and ^{1}H NMR spectral, and X-ray crytstallographic studies indicate that the new lariat ethers form stable complexes with alkali, alkaline earth, and transition metal ions and show unique selectivites for certain cations.

Results and Discussion

Synthesis of Ligands. Syntheses of 8-hydroxyquinoline-containing ligands **1**−**4** (Scheme 1) were accomplished by interaction of *N*,*N*′-bis(methoxymethyl)diazacrown ethers **5**−**7** or *N*-(methoxymethyl)aza-18-crown-6 (**8**) with 5-chloro-8-hydroxyquinoline (CHQ) in refluxing benzene. We have used this special Mannich reaction for the functionalization of azacrown ethers by other phenol groups.[7] Commercially available 5-chloro-8-hydroxyquinoline was used instead of 8-hydroxyquinoline because the chlorine blocks position 5 of the quinoline ring. Although attack *ortho* to the OH group is preferred in this electrophilic aromatic substitution reaction, we used the *para*-substituted material to avoid any minor products. Intermediate **5** has been described.[8] Intermediates **6** and **7** were

(5) (a) Stary, J. *The Solvent Extraction of Metal Chelates;* Pergamon Press: New York, 1964. (b) Sandell, E. B.; Onishi, H. *Photometric Determination of Traces of Metals*, 4th ed.; John Wiley & Sons: New York, 1978; p 415. (c) Welcher, F. J. *8-Hydroxyquinoline in Organic Analytical Reagents;* Van Nostrand Reinhold: Princeton, NJ, 1947; Vol. 1, p 264. (d) Gordon, L.; Salutsky, M. L.; Willard, H. H. *Precipitation from Homogeneous Solution;* John Wiley & Sons: New York, 1959.

(6) Zhang, X. X.; Bordunov, A. V.; Bradshaw, J. S.; Dalley, N. K.; Kou, X.; Izatt, R. M. *J. Am. Chem Soc.* **1995**, *117*, 11507.

(7) (a) Lukyanenko, N. G.; Pastushok, V. N.; Bordunov, A. V. *Synthesis* **1991**, 241. (b) Lukyanenko, N. G.; Pastushok, V. N.; Bordunov, A. V.; Vetrogon, V. I.; Vetrogon, N. I., Bradshaw, J. S. *J. Chem. Soc., Perkin Trans. 1* **1994**, 1489.

(8) (a) Bogatsky, A. V.; Lukyanenko, N. G.; Pastushok, V. N.; Kostyanovsky, R. G. *Dokl. Acad. Nauk SSSR* **1982**, *265*, 619; *Chem. Abstr.* **1982**, *97*, 216146. (b) Bogatsky, A. V.; Lukyanenko, N. G.; Pastushok, V. N.; Kostyanovsky, R. G. *Synthesis* **1983**, 992.

Scheme 2. Preparation of Azacrown Ether Ligands **10**, **11**, and **14**−**16** with 5-Chloro-8-hydroxy- and 5-Chloro-8-methoxyquinoline Side Arms

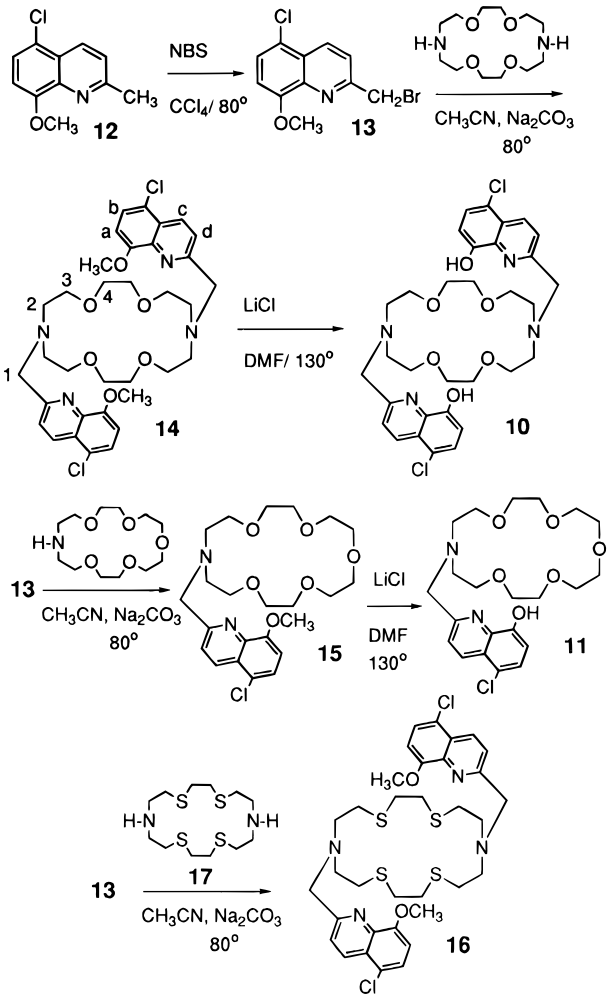

obtained by treatment of diaza-21-crown-7 or diaza-24-crown-8 with a methanol solution of formaldehyde. These intermediates were used in the next step without isolation. 4-Chlorophenol-containing **9** was synthesized in the same manner as **1**−**3** in order to compare the complexing abilities of **9** and **1**.

Different positioning of the coordinating sites can dramatically change the complexing properties of a ligand. Ligands **1**−**4** have the CHQ groups attached through position 7 of the CHQ ring. Bis(CHQ-substituted)diaza-18-crown-6 (**10**) and mono-(CHQ-substituted)aza-18-crown-6 (**11**), which have the CHQ groups attached through position 2 of the quinoline ring (pyridine portion), were also prepared (see Scheme 2). Ligands **1** and **10** differ only by reversing the attachment to quinoline from position 7 to position 2.

The 5-chloro-8-methoxy-2-methylquinoline (**12**) needed to prepare **10** and **11** was synthesized as described[9] using the Doebner−Miller reaction (condensation of 2-amino-4-chloroanisole with paraldehyde in acid). Key intermediate **13** was prepared by bromination of **12** with *N*-bromosuccinimide in refluxing CCl_4. Bromomethyl compound **13** was used to alkylate diaza-18-crown-6 and aza-18-crown-6 to give methoxy derivatives **14** and **15**, respectively. Ligand **14** formed a solid complex with sodium bromide which facilitated its purification.

Most of the reported methods for cleavage of the methoxy protecting groups are not suitable for compounds **14** and **15**. Reduction by $LiAlH_4$ in tetrahydrofuran (THF) was unsuccessful. We did not try LiI in pyridine or $NaSC_2H_5$ due to the possibility for nucleophilic substitution of the chlorine in the quinoline. Macrocycles **10** and **11** were prepared by using LiCl in dimethylformamide (DMF) to cleave the methyl groups.

We attempted to prepare the sulfur-containing analogue of **10**. The methoxy derivative of the tetrathia analogue of **10** (**16**) was prepared by treating diazatetrathia-18-crown-6 with **13** (Scheme 2). Unfortunately, the demethylated product of **16** could not be isolated.

Stabilities of Complexes. Interactions of CHQ and substituted ligands **1**−**3**, **9, 10** and **14** with various cations have been evaluated in methanol by a calorimetric titration technique.[10] For complexation of transition metal ions and Mg^{2+} with CHQ-containing ligands, deprotonation of CHQ substituents has to be considered in order to optimize the fitting process between experimental and calculated heat data. CHQ exhibits very weak interactions with K^+ and Mg^{2+} (see Table 1). However, **1**, with two attached CHQ groups, forms stable complexes with these cations with log *K* values of 3.39 for K^+ and 6.82 for Mg^{2+}. Compared with the parent macrocycle diaza-18-crown-6 (DA18C6),[11] these new hydroxyquinoline-containing crowns show increased binding constants at 25 °C in methanol for most metal cations. For example, the log *K* value for the K^+−DA18C6 interaction in methanol is 1.83 as determined by titration calorimetry at 25 °C,[11b] while log *K* values for K^+ interaction with **1**−**3**, **10**, and **14** under the same conditions are 3.01−6.61. This increase in log *K* is attributed to an enthalpic effect. Enthalpy changes for the CHQ-substituted crown interaction with the cations are more favorable than those for the DA18C6 interaction with the same cations[11b,c] suggesting that the hydroxyquinoline groups as well as the parent macroring bind with the cations.

Ligands **1**−**3**, with CHQ attached through position 7 of the quinoline ring (next to the OH group), form more stable complexes with transition metal ions than with alkali metal ions and Ba^{2+} (see Table 1). However, when CHQ is attached to the macroring through position 2 of the quinoline ring (next to the quinoline nitrogen), the resulting ligands **10** and **14** exhibit strong interactions with K^+ and Ba^{2+} but decreased interactions with the transition metal ions as compared with **1**−**3**. Hydroxy groups of **1**−**3**, and **9** can form intramolecular hydrogen bonds with the azacrown nitrogens (Figure 3a; see also X-ray Crystal Structures). Deactivation of crown nitrogens by hydrogen bonding with the OH groups would weaken interaction with the alkali metal cations. This last effect has been demonstrated by phenol-containing bis(azacrown ethers)[7b] and 2-hydroxy (Figure 3b) and 2-methoxy (Figure 3c) derivatives of dibenzyldiaza-18-crown-6.[1b] The 2-methoxybenzyl-substituted diazacrown formed stronger complexes with Na^+ and K^+ (log $K = 3.65$ and 4.94, respectively) than the (2-hydroxybenzyl)-diazacrown ether (log $K = 2.40$ and 2.59, respectively).[1b] The nitrogen atoms in the crown ether ring of **10** are not involved in intramolecular hydrogen bonding (see X-ray Crystal Struc-

(9) Weizmann, M.; Bograchov, E. *J. Am. Chem. Soc.* **1947**, *69*, 1222.

(10) (a) Oscarson, J. L.; Izatt, R. M. In *Physical Methods of Chemistry: Determination of Thermodynamic Properties;* Rossiter, B. W., Baetzoid, R. C., Eds.; John Wiley & Sons: New York, 1992; Vol. VI, Chapter 7. (b) Izatt, R. M.; Wu, G. *Thermochim. Acta* **1989**, *154*, 161−166. (c) Eatough, D. J.; Izatt, R. M.; Christensen, J. J. In *Biochemical and Clinical Applications of Thermometric and Thermal Analysis*; Jespersen, N. D., Ed.; Elsevier Science: New York, 1982; Chapters 2 and 7.

(11) (a) Gatto, V. J.; Arnold, K. A.; Viscariello, A. M.; Miller, S. R.; Gokel, G. W. *Tetrahedron Lett.* **1986**, *27*, 327. (b) Buschmann, H.-J. *Inorg. Chim. Acta* **1986**, *125*, 31. (c) Buschmann, H.-J. *J. Solution Chem.* **1986**, *15*, 453. (d) Buschmann, H.-J. *Inorg. Chim. Acta* **1985**, *108*, 241. (e) Kashanian, S.; Shamsipur, M. *Inorg. Chim. Acta* **1989**, *155*, 203.

Table 1. log *K*, Δ*H* (kJ/mol), and *T*Δ*S* (kJ/mol) Values[a] for Interactions of Macrocyclic Ligands with Cations in Methanol at 25.0 °C

ligand	cation	log *K*	Δ*H*	*T*Δ*S*	ligand	cation	log *K*	Δ*H*	*T*Δ*S*
CHQ	K^+	*b*			**9**	Na^+	-2.85 ± 0.03[e]	-16.0 ± 0.6	0.3
	Mg^{2+}	*b*				K^+	2.76 ± 0.04[e]	-24.1 ± 0.5	-8.4
	Cu^{2+}	(brown precipitate; thermodynamic quantities were not evaluated				Cs^+	*b*		
1	H^+ (1)	12.1 ± 0.3	-46.7	22.4		Mg^{2+}	*b*		
	H^+ (2)	8.15 ± 0.20	-50.3	-3.8		Ca^{2+}	4.48 ± 0.07[7e]	3.3 ± 0.5	22.3
	Na^+	2.89 ± 0.05	-14.1 ± 0.8	2.4		Sr^{2+}	<2[e]		
	K^+	3.39 ± 0.03	-24.4 ± 0.7	-5.0		Ba^{2+}	3.52 ± 0.06[e]	-32.3 ± 0.5	-12.2
	Cs^+	*b*				Zn^{2+}	4.21 ± 0.08	-44.7 ± 0.8	-20.7
	Mg^{2+}	6.82 ± 0.09[c]	-2.5 ± 0.6[c]	36.4		Cu^{2+}	4.14 ± 0.04	-64.3 ± 0.8	-40.7
	Ca^{2+}	5.31 ± 0.06[c]	-3.5 ± 0.4[c]	26.8		Co^{2+}	2.27 ± 0.04	-14.4 ± 0.7	-1.5
	Sr^{2+}	4.43 ± 0.08	13.2 ± 0.8	38.5	**10**	H^+ (1)	12.9 ± 0.3	-44.6	29.0
	Ba^{2+}	3.60 ± 0.05	-11.6 ± 0.5	8.9		H^+ (2)	8.25 ± 0.20	-47.8	-0.7
	Zn^{2+}	5.12 ± 0.04	-114 ± 3	-85		Na^+	3.74 ± 0.01[e]	-26.4 ± 0.3	-5.1
	Cu^{2+}	10.1 ± 0.1[c,d]	-92.5 ± 0.6	-34.9		K^+	6.61 ± 0.03[c,e]	-58.1 ± 0.1	-20.4
	Co^{2+}	5.14 ± 0.07	-91.1 ± 0.8	-61.8		Cs^+	2.70 ± 0.08[e]	-36.9 ± 0.8	-21.5
	Ni^{2+}	11.4 ± 0.5[c]	-94.7 ± 0.8	-29.6		Mg^{2+}	*b*		
2	Na^+	3.26 ± 0.02	-9.9 ± 0.4	8.7		Ca^{2+}	4.71 ± 0.05[e]	-25.2 ± 0.7	1.7
	K^+	3.01 ± 0.01	-29.4 ± 0.3	-12.2		Sr^{2+}	4.67 ± 0.04[e]	-24.6 ± 0.3	2.1
	Mg^{2+}	*b*				Ba^{2+}	12.2 ± 0.4[c,e]	-76.1 ± 0.7	-6.5
	Ca^{2+}	1.86 ± 0.08	-33.8 ± 0.8	-23.2		Zn^{2+}	(yellow precipitate; thermodynamic quantities were not evaluated)		
	Sr^{2+}	3.75 ± 0.05	15.4 ± 0.6	36.8		Cu^{2+}	4.7 ± 0.2[d]	-116 ± 4	-89
	Ba^{2+}	3.81 ± 0.09	-6.6 ± 0.7	15.1		Co^{2+}	4.8 ± 0.5	-70.8 ± 1.8	-43.4
	Cu^{2+}	>10[c]				Ni^{2+}	>5.5		
	Ni^{2+}	>10[c]			**14**	Na^+	3.06 ± 0.02	-12.1 ± 0.6	5.4
3	Na^+	2.28 ± 0.08	-7.9 ± 0.9	5.1		K^+	5.3 ± 0.2	-40.9 ± 0.3	-10.6
	K^+	3.41 ± 0.01	-35.5 ± 0.2	-16.0		Cs^+	3.86 ± 0.02	-40.5 ± 0.4	-18.5
	Mg^{2+}	*b*				Mg^{2+}	*b*		
	Ca^{2+}	2.22 ± 0.07	-20.7 ± 0.5	-8.0		Ca^{2+}	*b*		
	Sr^{2+}	3.68 ± 0.05	8.9 ± 0.7	29.9		Sr^{2+}	*b*		
	Ba^{2+}	4.48 ± 0.08	-4.7 ± 0.5	20.9		Ba^{2+}	5.6 ± 0.1	-29.1 ± 0.1	2.9
	Cu^{2+}	>5.5				Zn^{2+}	(white precipitate; thermodynamic quantities were not evaluated)		
	Ni^{2+}	>10[c]				Cu^{2+}	(brown precipitate; thermodynamic quantities were not evaluated)		
9	H^+ (1)	11.6	-28.4	37.8		Co^{2+}	2.86 ± 0.02	37.1 ± 0.8	53.4
	H^+ (2)	8.56	-30.4	18.5		Ni^{2+}	2.3 ± 0.2	29.6 ± 3.2	42.7

[a] Values are the averages taken from two to four determinations, except for the Δ*H* values for protonation reactions and protonation constants of **9** (due to limited amount of **9**). Uncertainties are given as standard deviations. Protonation constants were determined by a potentiometric titration. The consecutive protonation process is indicated by (1) and (2). [b] No measurable heat other than heat of dilution indicating that Δ*H* and/or log *K* is small. [c] Quantities were determined by competitive calorimetric titration. [d] Precipitation happened after the solutions were mixed for about 40 min. [e] Reference 6.

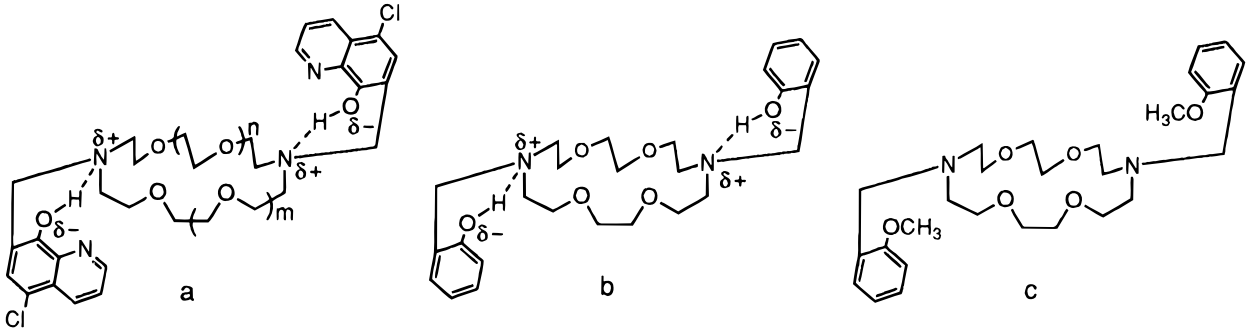

Figure 3. Diaza-18-crown-6 functionalized with aromatic side arms.

tures). Ligand **14** also has free azacrown nitrogens. Thus, the diazacrown portions of **10** and **14** are able to interact effectively with alkali metal cations.

Lariat azacrown **9** has two chlorophenols instead of two CHQs as its pendant arms. Log *K* values for the complexes with **9** are lower than those for the complexes with **1**. The most significant decrease in log *K* is observed for Cu^{2+}. Ligand **9** forms a less stable complex with Cu^{2+} than does **1** by 6 orders of magnitude, indicating that the quinoline derivatives are much better functional groups for cation binding and selectivity than phenol derivatives. Ligand **10** forms more stable complexes with most studied cations than does **14**. Probably, the greater negative charge density of the hydroxy oxygens of free **10** (due to intermolecular hydrogen bonds; see X-ray Crystal Structures) makes them more effective complexing sites than the OCH_3 groups of **14**. Moreover, the greater ability of the OH functions to donate electrons into the quinoline aromatic system could increase the interaction of the quinoline nitrogens with cations. Compound **10** forms the most stable complex with Ba^{2+}. The log *K* value for formation of the **10**$-Ba^{2+}$ complex is near to that for formation of the cryptand [2.2.2]$-Ba^{2+}$ complex.[12] This strong interaction is a result of the Ba^{2+} acting as a template to bring the two quinoline rings into close proximity.[6] The resulting intramolecular association between the two quinoline rings causes a cryptand-like structure to form. This effect will be discussed below.

Selectivity of Cations. Ligands **1** and **2** show a high selectivity for Cu^{2+} and Ni^{2+} over other cations. Compound **1** not only shows high Mg^{2+}/Na^+ and Mg^{2+}/K^+ selectivity but it

(12) (a) Chantooni, M. K., Jr.; Kolthoff, I. M. *J. Solution Chem.* **1985**, *14*, 1. (b) Arnaud-Neu, F.; Yahya, R.; Schwing-Weill, M. J. *J. Chim. Phys. Phys.-Chim. Biol.* **1986**, *83*, 403.

also selectively binds Mg^{2+} over Ca^{2+} and Zn^{2+} by a factor greater than 32 ($\Delta \log K > 1.5$). This special selectivity of **1**, together with the specific UV response of the **1**−Mg^{2+} complex (see below for UV results), makes ligand **1** a possible indicator for Mg^{2+} in biological samples. It is of interest that log *K* values for formation of the alkaline earth metal cation complexes with **1** decrease with increasing cation radius, i.e., $Mg^{2+} > Ca^{2+} > Sr^{2+} > Ba^{2+}$. In contrast, compounds **2** and **3** have the sequence of $Mg^{2+} < Ca^{2+} < Sr^{2+} < Ba^{2+}$. This observation demonstrates the substantial influence of the size of the macrocyclic ring on complex formation. The fact that **9** (Scheme 1) exhibits no special selectivity among the metal cations indicates the important role of the hydroxyquinoline substituent on cation selectivity. Selectivity for K^+ over Na^+ and Cs^+ and of Ba^{2+} over other alkaline earth metal ions is demonstrated by **14**. Ligand **10** exhibits an excellent selectivity for Ba^{2+} over all other cations studied. Among the alkali metal ions, **10** has a high selectivity for K^+.

Thermodynamic Quantities. Formation of Zn^{2+} and transition metal (Cu^{2+}, Co^{2+}, and Ni^{2+}) complexes with these hydroxyquinoline- and phenol-containing azacrown ethers is enthalpy driven. Except for complexes with **14,** the entropy changes are unfavorable. Similarly, K^+ and Cs^+ complexes are stabilized by favorable enthalpy changes. In most cases, the alkaline earth complexes are stabilized by both enthalpic and entropic effects. The high stability of Mg^{2+} and Ca^{2+} complexes with **1** results mainly from an entropic effect.

Compounds **1**−**3** have the same CHQ arms but different macroring sizes. $-\Delta H$ values decrease for Na^+ interactions but increase for K^+ interactions with the increasing size of the macroring. Among Na^+ and K^+ complexes of these ligands, the largest log *K* value is observed for the **2**−Na^+ complex and the smallest log *K* value for the **2**−K^+ one. Entropic effects play an important role in the stability of the Na^+ complexes. The **2**−Na^+ interaction shows the most favorable entropic change ($T\Delta S = 8.7$ kJ/mol) among the three ligands, resulting in a stable complex. In the case of the K^+ complexes, although the large macroring displays a large conformational entropy loss ($T\Delta S$ values have the sequence of **1** > **2** > **3**), the more symmetric **1** and **3** bind K^+ better than the less symmetric **2**.

Ba^{2+} complexes with **9** and **10** exhibit negative $T\Delta S$ values, while all other Ba^{2+} complexes in this study have positive $T\Delta S$ values. The very high stability of the Ba^{2+}−**10** complex results from a favorable enthalpy change ($\Delta H = -76.1$ kJ/mol). The opposite sign for the $T\Delta S$ value for the Ba^{2+}−**10** complex when compared to complexes with the other CHQ-substituted ligands may indicate a large difference in their complex structures. Coordination with Ba^{2+} by two CHQ rings on the same side of the macroring of **10** would result in a large conformational change of the ligand, leading to the negative $T\Delta S$ value. The crystal structure of the Ba^{2+}−**10** complex shows that the two CHQ units do bind the Ba^{2+} on the same side of the macroring, while the free ligand has side arms on opposite sides of the diazacrown (see X-ray Crystal Structures).[6] The CHQ rings of **1**−**3** may bind with Ba^{2+} from the opposite sides of the macroring since such a coordination would result in a small conformational change for the ligands and, therefore, small entropic losses. The negative $T\Delta S$ value for Ba^{2+}−**9** complexation indicates that **9** may also experience a large conformational change during complexation.

The large $-\Delta H$ values associated with the interactions of Cu^{2+} and Ni^{2+} with **1** and Ba^{2+} with **10** indicate that enthalpy changes make important contributions in forming these very stable complexes. The high stability of the K^+ complexes with **10** and **14** also results from favorable enthalpy changes. Although Zn^{2+}−**1**, Co^{2+}−**1**, Co^{2+}−**10,** and Cu^{2+}−**10** interactions exhibit large $-\Delta H$ values, the binding constants are not very large because of unfavorable entropy changes (large $-T\Delta S$ values). A host−guest interaction having large $-\Delta H$ and small $-T\Delta S$ values indicates strong binding with a small conformational change and, consequently, results in a very stable complex. On the other hand, an interaction having a large $-\Delta H$ value may not result in a stable complex if there is a large conformational entropic loss. For example, the large $-\Delta H$ values for the interaction of **1** with Zn^{2+} and the transition metal ions indicate strong binding between **1** and the cations. Among them, **1** selectively binds Cu^{2+} and Ni^{2+} due to smaller conformational entropic losses as compared with those of Zn^{2+} and Co^{2+}. This observation suggests that **1** fits Cu^{2+} and Ni^{2+} better than Zn^{2+} and Co^{2+}.

UV−Visible Spectra. The UV−visible spectral data are listed in Table 2. Typical absorption spectra of free and complexed ligands (**1** and **10**) are shown in Figures S6 and S7 in the Supporting Information. Figure S8 (Supporting Information) shows the spectra of the Mg^{2+} complexes of CHQ, **1,** and **10.** All CHQ-substituted diazacrown ethers exhibit three absorption bands which originate from their aromatic ring substituents. Compared with CHQ, the spectra of the quinoline groups of the diazacrown ethers have changes in both λ_{max} and molar absorptivity values. CHQ-substituted crown ethers **1**, **10**, and **14** have strong absorptions at 204 and 247−249 nm. A strong absorption is also observed for **9** at 204 nm, but the second strong peak is at 231 nm. The third absorption is weaker than the former two bands, and its position is different for different ligands (from 286 nm for **9** to 332 nm for **1**; see Table 2). This weak band is more sensitive to cation complexation than the two strong bands. Formation of stable complexes (K^+ and Ba^{2+} with **10** and Ca^{2+} with **1** and **10**) results in an appreciable shift of the third (weak) band of the ligands (Table 2). Na^+ has little effect on the UV−visible spectra of the ligands, which is consistent with the low log *K* values in this case. Compound **14** exhibited little or no change in its UV−visible spectrum by complexation, suggesting a small structural change of the methoxyquinoline rings before and after complexation.

Among the alkali and alkaline earth metal cations, the UV−visible spectra of the Mg^{2+} complexes are unique. Not only do the third absorption bands of **1** (at 332 nm) and **10** (at 319 nm) shift appreciably (bathochromic shifts of 9 and 8 nm to 341 and 327 nm, respectively) but also new peaks at 265 and 268 nm appear (Table 2). The new peaks ($\epsilon = 10^3-10^4$ M^{-1} cm^{-1}) probably originate from a charge transfer process since neither Mg^{2+} nor the ligands have absorption in that region. The absorption intensity of the new peak at 265 nm for the Mg^{2+}−**1** complex ($\epsilon = 6.0 \times 10^4$ M^{-1} cm^{-1}) is increased greatly as compared with that for Mg^{2+}−CHQ (λ_{max} 262 nm, $\epsilon = 9.2 \times 10^3$ M^{-1} cm^{-1}) and with that for complex Mg^{2+}−**10** (λ_{max} 268 nm; a shoulder peak; $\epsilon = 1.7 \times 10^4$ M^{-1} cm^{-1}). This special enhanced peak in the Mg^{2+}−**1** complex is in agreement with the large log *K* value in this case. Because the other alkali and alkaline earth metal ions do not have such an absorption, this unique UV peak at 265 nm may provide a promising method for Mg^{2+} analysis in samples where alkali and other alkaline earth metal ions are present. In order to explore the possibility of using **1** for Mg^{2+} analysis, we obtained the UV spectrum of **1** at a low Mg^{2+} concentration (1.2×10^{-5} M). The spectrum at this low concentration was the same as that reported in Table 2.

CHQ-substituted crown ethers **1** and **10** exhibit significant changes in their UV−visible spectra upon complexation with

Table 2. UV-Visible Spectral Data Valid in Methanol for Several Ligands and Their Metal Ion Complexes

(a) Absorption Maxima (λ_{max}, nm) and Molar Absorptivity Values (ϵ) of Ligands

ligand	λ_{max} (ϵ, M^{-1} cm^{-1})	λ_{max} (ϵ, M^{-1} cm^{-1})	λ_{max} (ϵ, M^{-1} cm^{-1})
1	204 (8.3×10^4)	249 (1.2×10^5)	332 (1.1×10^4)
9[c]	204 (3.7×10^4)	231 (1.6×10^4)	286 (4.2×10^3)
10[c]	204 (6.0×10^4)	249 (7.4×10^4)	319 (6.6×10^3)
14	204 (1.0×10^5)	247 (1.1×10^5)	311 (1.2×10^4)
CHQ	203 (2.4×10^4)	245 (3.6×10^4)	329 (3.7×10^3)

(b) Absorption Maxima (λ_{max}, nm)[a] of the Ligands upon Complexation with the Metal Ions[b]

ligand	Na^+	K^+	Mg^{2+}	Ca^{2+}	Ba^{2+}	Co^{2+}	Ni^{2+}
1	205	205	203, 248	203	206	203, 262	208, 265
	249	249	265, 341	250	248	347, 395	348, 400
	332	333	397	338	333		
9	206, 231[c]	206, 231[c]	203, 231		207, 231[c]		
	286[c]	286[c]	286		290[c]		
10	207	207	204, 249	204	207	205, 264	224, 247
	248[c]	245[c]	268 (sh)	248	250[c]	344, 413	269, 347
	318	315[c]	327	324	316[c]		419
14		205, 247	204, 247		205, 249		214, 248
		310	311		311		311
CHQ			203, 245				
			262, 330				

[a] The metal ion concentrations were 40 times in excess to ensure a complete complexation. [b] λ_{max} values below 230 nm for Ni^{2+} complexes are a combination of the complex and $Ni(NO_3)_2$, which has a strong absorption at 208 nm ($\epsilon = 1.4 \times 10^4$ M^{-1} cm^{-1}). [c] Reference 6.

Table 3. Proton Chemical Shifts δ (ppm) of Complexed and Free Hydroxyquinolinocrown Ethers and Cation-Induced Shifts (CIS (Hz), Values in Parentheses) in 2/8 $CDCl_3/CD_3OD$ at 25.0 °C[a]

	aromatic protons				methylene protons			
species	H_a	H_b	H_c	H_d	H_1	H_2	H_3	H_4
1	8.835	7.579	8.526	7.466	4.058	2.963	3.645	3.764
1$-Na^+$	8.711 (24.8)	7.491 (17.6)	8.337 (37.8)	7.454 (2.4)	3.841 (43.4)	2.837 (25.2)	3.365 (56.0)	3.680 (16.8)
1$-K^+$	8.767 (13.6)	7.608 (−5.8)	8.545 (−3.8)	7.567 (−20.2)	3.841 (43.4)	2.759 (40.8)	3.400 (49.0)	3.618 (29.2)
1$-Mg^{2+}$	8.684 (30.2)	7.677 (−19.6)	8.284 (48.4)	7.562 (−19.2)	3.761[b] (59.4)	3.133[b] (−34.0)	3.435[b] (42.0)	3.595 (33.8)
1$-Ba^{2+}$	8.837 (−0.40)	7.756 (−35.4)	8.688[b] (−32.4)	7.684 (−43.6)	4.057[c]	2.898[b] (13.0)	3.711[b] (−13.2)	3.843[b] (−15.8)
9	6.712	7.087	7.052	−	3.796	2.833	3.600	3.674
9$-K^+$	6.774 (−12.4)	7.158 (−14.2)	7.119 (−13.4)	−	3.678[c]	2.732 (20.2)	3.503 (19.4)	3.637 (7.40)
9$-Ba^{2+}$	6.898 (−37.3)	7.209 (−24.5)	7.175 (−24.6)	−	3.818[c]	2.801[b] (6.4)	3.747[b] (−29.4)	3.791[c]
10	7.027	7.444	8.426	7.724	4.120	2.982	3.597	3.711
10$-Na^+$	6.887 (28.0)	6.998 (89.2)	7.948 (95.6)	7.381 (68.6)	4.004 (23.2)	2.817 (33.0)	3.750[c]	3.793[c]
10$-K^+$	6.696 (66.2)	6.985 (91.8)	7.911 (103.0)	7.170 (110.8)	4.021 (19.8)	2.801[b] (36.2)	3.764[c]	3.795[c]
10$-Ba^{2+}$	6.523 (100.8)	7.000 (88.8)	8.238 (37.6)	7.513 (42.2)	4.193[c]	2.372[c]	3.720[c]	3.819[c]
14	7.061	7.483	8.413	8.006	4.061	2.919	3.618	3.694
14$-K^+$	6.355 (141.2)	7.185 (59.6)	8.315 (19.6)	7.471 (107.0)	4.110 (−9.8)	2.860 (11.8)	3.621 (−0.6)	3.744 (−10.0)
14$-Ba^{2+}$	6.252 (161.8)	7.241 (48.4)	8.594 (−36.2)	7.725 (56.2)	3.969[b] (18.4)	2.880[b] (7.8)	3.324 (58.8)	3.920[c]

[a] Concentrations of the ligands were 0.01 M and those of metal ions 0.02−0.05 M. The chemical shifts are referred to internal Me_4Si. CIS (Hz) $= 200[\delta_{lig}$ (ppm) $- \delta_{complx}$ (ppm)]. The "−" refers to downfield and the positive value in parentheses upfield shifts. [b] The peak is broadened. [c] The peak shape has a large change as compared to that of the free ligand.

the transition metal ions (Co^{2+} and Ni^{2+}) (see Table 2). A new absorption band can be observed in the vicinity of 400 nm which is probably a charge transfer band. The maximum absorption of the ligands is shifted in most cases, and the Ni^{2+}−**10** complex shows a new peak at 269 nm. Thus, the UV−visible spectral data indicate an appreciable interaction of the CHQ groups with cations, especially with Mg^{2+}, Ni^{2+}, and Co^{2+}, which are able to form chelate complexes with **1** and **10**.

^{1}H NMR Spectra. Chemical shifts in the proton NMR spectra of the ligands and their complexes in a 2/8 $CDCl_3/CD_3OD$ solvent mixture are listed in Table 3. Upon complexation with the metal cations, all proton signals of the ligands undergo chemical shift changes of varying magnitudes, indicating interaction of the cations with both macroring and CHQ moieties.[13] Similar changes in the ^{1}H NMR spectra for **10** and its complexes with Na^+, K^+, and Ba^{2+} in dimethyl sulfoxide (DMSO) were reported previously.[6] ^{1}H NMR spectra of ligands **1** and **10** and their Na^+ and Ba^{2+} complexes are shown in Figures S9 and S10 in the Supporting Information. Large changes in ligand NMR spectra can be seen upon complexation with the cations. Broadened, merged, and split signals of the macroring protons are the result of anisotropic effects and the reduction of conformational flexibility by encapsulation of a cation in the macroring.[13e]

The degrees of cation-induced shifts (CIS) are different for **1, 9, 10,** and **14**. Not only does a direct interaction of the cations with the macroring and aromatic fragments affect the CIS values, but also complex formation makes a different environment for the protons compared with those of the free ligands. The direction of CIS of the aromatic protons provides some insight into cation binding and conformation of the complexes. ^{1}H

(13) (a) Live, D.; Chan, S. I. *J. Am. Chem. Soc.* **1976**, *98*, 3769. (b) Takai, Y.; Okumura, Y.; Takahashi, S.; Sawada, M.; Kawamura, M.; Uchiyama, T. *J. Chem. Soc. Chem. Commun.* **1993**, 53. (c) Li, Y.; Echegoyen, L.; Martinez-Diaz, M. V.; de Mendoza, J.; Torres, T. *J. Org. Chem.* **1991**, *56*, 4193. (d) Tsukube, H.; Sohmiya, H. *J. Org. Chem.* **1991**, *56*, 875. (e) Seel, C.; Vögtle, F. In *Perspectives in Coordination Chemistry*, Williams, A. F.; Floriani, C.; Merbach, A. E., Eds.; VCH Publishers Inc.: New York, 1992; p 47. (f) Izatt, R. M.; Zhu, C. Y.; Dalley, N. K.; Curtis, J. C.; Kou, X.; Bradshaw, J. S. *J. Phys. Org. Chem.* **1992**, *5*, 656.

Table 4. Proton Chemical Shifts δ (ppm) of Neutral and Deprotonated Lariat Ethers and Based-Induced Shifts (BIS (Hz), Values in Parentheses) in 2/8 CDCl3/CD_3OD at 25.0 °C[a]

	aromatic protons				methylene protons			
species	H_a	H_b	H_c	H_d	H_1	H_2	H_3	H_4
1	8.835	7.579	8.526	7.466	4.058	2.963	3.645	3.764
1 + OH^-	8.675 (32.0)	7.396 (36.6)	8.367 (31.8)	7.611 (−29.0)	3.927 (26.2)	2.855 (21.6)	3.619 (5.2)	3.731 (6.6)
9	6.712	7.087	7.052	−	3.796	2.833	3.600	3.674
9 + OH^-	6.636 (15.1)	7.115 (−5.6)	6.948 (20.8)	−	3.738 (11.6)	2.839 (−1.2)	3.625 (−5.0)	3.680 (−1.2)
10	7.027	7.444	8.426	7.724	4.120	2.982	3.597	3.711
10 + OH^-	6.718 (61.8)	7.238 (41.2)	8.309 (23.4)	7.711 (2.6)	4.009 (22.2)	2.911 (14.2)	3.614 (−3.4)	3.682 (5.8)
14	7.061	7.483	8.413	8.006	4.061	2.919	3.618	3.694
14 + OH^-	7.062 (−0.2)	7.482 (0.2)	8.409 (0.8)	7.007 (−0.2)	4.060 (0.2)	2.907 (2.4)	3.617 (0.2)	3.689 (1.0)

[a] The base was tetramethylammonium hydroxide ($(CH_3)_4N^+OH^-$ 0.05 M). Concentrations of the ligands were 0.01 M. The chemical shifts are referred to internal Me_4Si. BIS (Hz) = $200[\delta_{lig}$ (ppm) − $\delta_{lig\text{-}OH^-}$ (ppm)]. The "−" refers to downfield and the positive value in parentheses upfield shifts.

NMR experiments showed small downfield shifts of the aromatic protons of free quinoline, 8-quinolinol, 1-naphthol, naphthalene, and 5-chloro-8-hydroxyquinoline when metal ions (K^+ and Ba^{2+}) were added to their $CDCl_3/CD_3OD$ (2/8, v/v) solutions. This fact can be understood in terms of electron-donating interactions of aromatic compounds with cations, which results in a magnetic deshielding effect. The downfield shifts can be observed for aromatic protons of the **1** and **9** complexes with K^+ and Ba^{2+} (Table 3), indicating coordination of CHQ moieties of **1** and chlorophenol moieties of **9** with the cations.

As can be seen from Table 3, however, large upfield shifts occur for aromatic protons of **10** and **14** upon complexation. This cannot be understood from the electron-donating point of view. Two factors were considered as causes of the upfield shifts of the quinoline protons. First, deprotonation of the hydroxyquinoline groups increases the electron density on the quinoline ring and causes an upfield shift of the aromatic protons. This point can be seen by the ^1H NMR spectra of the CHQ-substituted macrocycles in a base solution in which the hydroxy groups should be completely deprotonated. Significant upfield shifts for most aromatic protons of **1, 9**, and **10** were observed when $(CH_3)_4N^+OH^-$ was added to the solutions of these compounds (see Table 4). On the other hand, the upfield shifts of aromatic proton signals of **14** upon its complexation are not caused by deprotonation since **14** has no ionizable protons. No appreciable proton shifts for **14** were observed by adding strong base (Table 4). In addition, several CIS values for complexes of **10** with K^+ and Ba^{2+} are much larger (>100 Hz, Table 3) than the values of the chemical shifts induced by deprotonation in strong base solution (3−62 Hz, Table 4). We also did not observe changes in the UV spectra of **1** and **10** when they formed complexes with Na^+ (no deprotonation) in spite of appreciable upfield shifts of aromatic proton signals on the Na^+−**1** and Na^+−**10** complexes. Hence, there must be another factor which results in upfield shifts of the quinoline protons under these conditions. This could be a close approach and overlapping of two quinoline rings, which results in a magnetic shielding effect[14] and upfield shifts of the proton NMR signals. The large upfield shifts of quinoline protons observed for **10** and **14** complexes with K^+ and Ba^{2+} can be attributed to a π-stacking between the two quinoline units when binding the cation from the same side of the diazacrown ring (Figure 2a).[6] Similar upfield shifts were observed[15] when phenanthridine-substituted DA18C6 formed complexes with Na^+ and K^+. The structure of the K^+ complex with this latter ligand was proved by an X-ray crystal structure study. The structure had close one-side coordination (relative to the diazacrown ring) of the cation by the two phenanthridine moieties. In our case, the crystal structure of the Ba^{2+}−**10** complex (Figure 8) shows close coordination of Ba^{2+} by two hydroxyquinoline side arms on the same side of the diazacrown (Figure 2a). The overlapping of the two quinoline units has, in effect, formed a pseudoring, resulting in complexes having a cryptate-like structure.[6] We believe that only cations with the appropriate size can cause efficient overlapping of the two hydroxyquinoline rings. Therefore, the strongest interaction occurs with ions capable of bringing the hydroxyquinoline side arms together. In the case of compounds **10** and **14**, the highest log *K* values (see Table 1) were observed for K^+ and Ba^{2+} which have the proper size to stack the hydroxyquinoline moieties. Thus, ligands which show very high recognition do not need to be three-dimensional since a pseudo-three-dimensional structure can be formed during complexation of the lariat ether.[6] The close one-sided coordination could occur for the Na^+−**10**, K^+-**10**, Ba^{2+}−**10**, K^+−**14**, and Ba^{2+}−**14** complexes, since they exhibited large upfield shifts of the aromatic protons in their ^1H NMR spectra (see Table 3).

The downfield shifts of the signals for aromatic protons in the K^+−**1** and Ba^{2+}−**1** complexes could indicate a large distance between the hydroxyquinoline side arms. This situation could occur by (1) opposite side coordination (Figure 2b), (2) one-side coordination when the aromatic side arms are far from each other (Figure 2c), or (3) coordination of the cation with one side arm when the second arm is far away (Figure 2d). We observed positive $T\Delta S$ values for the Ba^{2+}−**1** complex as well as for the Ba^{2+}−**2** and Ba^{2+}−**3** complexes. These data and the downfield direction of CIS in the Ba^{2+}−**1** complex point to small conformational changes of the ligands during complexation and probably opposite-side coordination of Ba^{2+} by these ligands. Complexation as shown in Figure 2d was observed for the Ba^{2+}−**9** complex (see X-ray data). In the crystal structure, one of the chlorophenol moieties was not associated with the cation, but rather a DMF molecule occupied one of the Ba^{2+} coordination sites.

In the case of the **1**−Mg^{2+} complex, both aromatic and macroring ^1H NMR signals undergo appreciable shifts as compared to the free ligand (Table 3). These ^1H NMR signal changes show that Mg^{2+} interacts with both CHQ arms and the crown ether ring. Two CHQ protons (H_a and H_c) exhibited upfield shifts, while the other two (H_b and H_d) showed downfield shifts. The degrees of the CHQ proton shifts are not as large as those in the complexes with **10** and **14**, suggesting an opposite-side coordination of Mg^{2+} by ligand **1** (Figure 2b). A positive $T\Delta S$ value for **1**−Mg^{2+} complexation (36.4 kJ/mol; see Table 1) supports this point. The coordination of Mg^{2+} by both CHQ arms and the macroring can also be seen by a comparison

(14) Sanders, J. K. M.; Hunter, B. K. *Modern NMR Spectroscopy*; Oxford University Press: Oxford, U.K., 1987.
(15) Alihodžić, S.; Žinić, M.; Klaić, B.; Kiralj, R.; Kojić-Prodić, B.; Herceg, M.; Cimerman, Z. *Tetrahedron Lett.* **1993**, *34*, 8345.

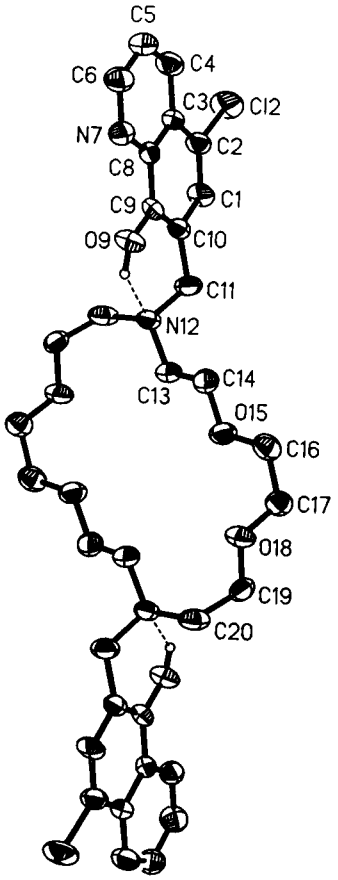

Figure 4. Computer drawing of **1** with all hydrogen atoms except those involved in hydrogen bonds omitted for clarity. Thermal ellipsoids were drawn at the 50% probability level.

of the thermodynamic data for the CHQ−Mg^{2+} and **1**−Mg^{2+} interactions. The log *K* value for interaction of Mg^{2+} with CHQ cannot be determined by the calorimetric method due to a very small heat of reaction, while Mg^{2+} forms a highly stable complex with **1** (log $K = 6.82$).

X-ray Crystal Structures. Crystal structures of ligand isomers **1** and **10** and the Ba^{2+}−**10** complex along with the structures of **9** and its Ba^{2+} complex, Ba^{2+}−**9**, have been determined by X-ray diffraction methods. Crystal data and experimental details for each structure are discussed in the Experimental Section. The crystal structures of both complexes include solvent molecules. The asymmetric unit of Ba^{2+}−**9** contains a water molecule and a DMF molecule, both of which are involved in the coordination of Ba^{2+}. The asymmetric unit of Ba^{2+}−**10** contains two chloroform molecules, one water molecule, and half of a disordered molecule located about an inversion center. This molecule could not be identified and is not included in the coordination of Ba^{2+}. The only solvent molecule in the Ba^{2+}−**10** complex that interacts with the cation is water.

Each of the free ligands, **1, 9**, and **10**, is located about a center of inversion. The structures of **1, 9**, and **10** are shown in Figures 4−6, respectively. These figures show the conformations of the three molecules and the atom labels. There are similarities between **1** and **9**. Both **1** and **9** contain intramolecular hydrogen bonds involving the phenol groups of the lariat arms in **9** and the hydroxy groups of the CHQ of the lariat arms in **1** and ring nitrogen atoms of the ligands. As a result of these intramolecular hydrogen bonds, each molecule is elongated along the N···N direction and exists as a monomer. The relationship of the aromatic rings of **1** and **9** to their respective crown rings is different. In **1,** the CHQ rings are extended away from the

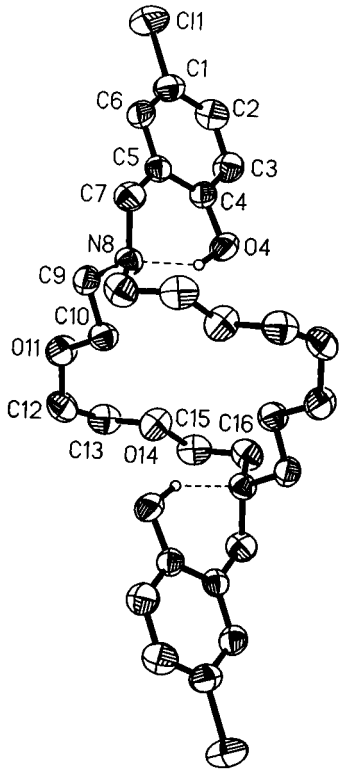

Figure 5. Computer drawing of **9** with all hydrogen atoms except those involved in hydrogen bonds omitted for clarity. Thermal ellipsoids were drawn at the 50% probability level.

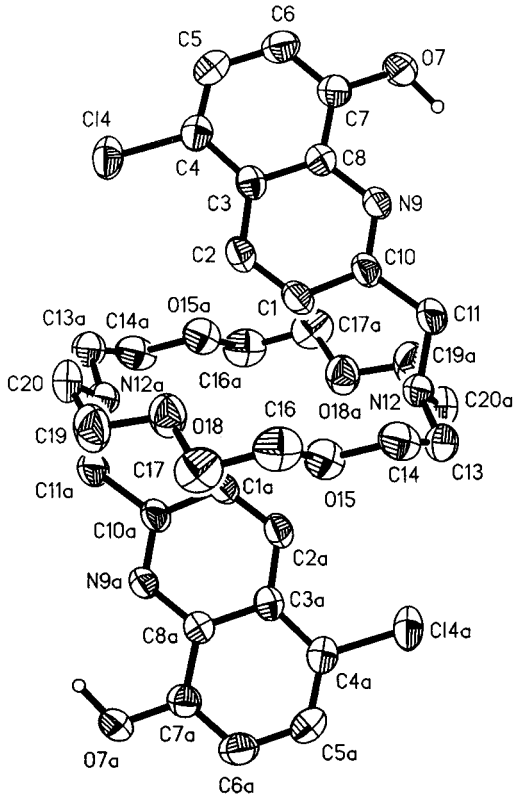

Figure 6. Computer drawing of one molecule of **10** with all hydrogen atoms except those involved in hydrogen bonds omitted for clarity. Thermal ellipsoids were drawn at the 50% probability level.

cavity of the crown ring, while, in **9**, the phenol rings are located on opposite sides of the cavity (see Figures 4 and 5).

As indicated above, **1** and **10** are structural isomers differing in that, in **1**, the phenol portions of the two 8-hydroxyquinolines are linked to the diaza-18-crown-6 nitrogens by carbon atoms,

Table 5. Hydrogen Bond Data and Short Donor−Acceptor Interatomic Distances in the Structures

compd	D	H	A	D···A (Å)	H···A (Å)	D−H···A (deg)	sym transl of A
1	O9	H9	N12	2.643(12)	1.93(5)[a]	138(1)[a]	*x*, *y*, *z*
9	O4	H4	N8	2.652(3)	1.75(5)	142(1)	*x*, *y*, *z*
10	O7	H7	N29	2.957(3)	2.00(5)	156(1)	*x*, *y*, *z*[b]
	O27	H27	N9	2.823(4)	1.97(5)	148(1)	*x*, *y*, *z*[b]
Ba^{2+}−**9**	O4	H4	Br1	3.275(11)	2.18(5)	167(1)	$1-x, y-0.5, 0.5-z$
	O32		Br2[c]	3.044(9)			$1-x, -y, -z$
	O37	H37A	Br1	3.334(10)	2.55(5)	147(1)	$-x, y-0.5, 0.5-z$
	O37	H37B	Br1	3.404(10)	2.46(5)	158(1)	*x*, *y*, *z*
Ba^{2+}−**10**	O7	H7	Br2	3.256(9)	2.59(5)	132(1)	$1+x, y, z$
	O38		Br2[c]	3.295(9)			*x*, *y*, *z*
	O43	H43A	Br1	3.433(11)	2.67(5)	127(1)	$1-x, 1-y, 1-z$
	O43	H43B	Br1	3.344(10)	2.29(5)	174(1)	$x-1, y, z$

[a] The estimated standard deviation values on distances and angles involving hydrogen atoms are estimated on the basis of past experience since the positions of the hydrogen atoms were not refined. [b] A is in the other independent molecule. [c] The D···A interatomic distances suggest the presence of a hydrogen bond, but it was not possible to obtain a position for the hydrogen atom involved.

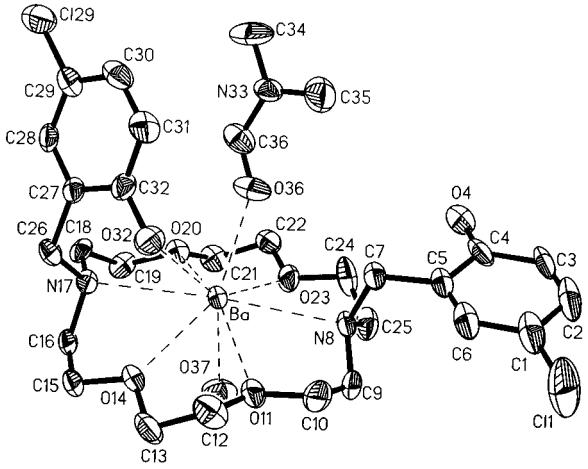

Figure 7. Computer drawing of Ba^{2+}−**9**, including the water and DMF ligands. The bromide ions and all hydrogen atoms are omitted for clarity. Thermal ellipsoids were drawn at the 40% probability level.

while in **10** the pyridine portions are closest to the crown nitrogen atoms (see Figures 4 and 6). Ligand **10** also differs from **1** and **9** in that its unit cell contains two chemically similar but crystallographically independent molecules. The two independent molecules are similar, so only one of them is shown in Figure 6. The figure also shows that, with the absence of intramolecular hydrogen bonding in **10**, the CHQ nitrogen atoms and hydroxy groups point away from the crown ring. The CHQ nitrogen atom and hydroxy group of one independent molecule form hydrogen bonds to the similar atom groupings of the other molecule, resulting in an interaction similar to base pairing that is found in many biologically significant molecules. The result is long chains of **10** molecules with alternating crystallographically independent molecules. Hydrogen bond data for **1, 9**, and **10** as well as for both Ba^{2+} complexes are listed in Table 5.

The properties of the solid Ba^{2+} complexes of **9** and **10** have been reported,[6] but few structural details were included. When the conformation of uncomplexed **9** (Figure 5) is compared with its conformation in Ba^{2+}−**9** (Figure 7), some significant conformational differences are apparent. In the Ba^{2+} complex both lariat arms are now on the same side of the cavity of the diaza crown ring. Interestingly, one of the phenol oxygens, O4, is not involved in the coordination of the cation (Ba^{2+}···O4 distance is 5.950 Å) or in a hydrogen bond with a nitrogen atom of the macrocycle (N8···O4 distance is 3.664 Å). Ba^{2+} is complexed by nine donor atoms (see Figure 7), as described previously.[6] The Ba^{2+}−donor atom interatomic distances in Ba^{2+}−**9** and Ba^{2+}−**10** are listed in Table 6. The shortest Ba−O distance listed (2.615(10) Å) is between Ba^{2+} and O36, the DMF oxygen atom. This distance is at least 0.1 Å shorter than any other Ba^{2+}···donor atom distance in either complex and indicates a strong cation···donor atom interaction. The location of O36 in the coordination sphere of Ba^{2+} suggests that the DMF molecule is located in the place that O4 would have occupied if it were coordinated to Ba^{2+}. It is possible that in the presence of a less polar solvent than DMF, both phenol oxygens would have interacted with Ba^{2+}.

Table 6. Ba^{2+}−Donor Atom Distances in the Two Complexes

Ba^{2+}−**9**		Ba^{2+}−**10**	
donor atom, D	Ba^{2+}···D, Å	donor atom, D	Ba^{2+}···D, Å
		$O7_{ph}$	3.005 (7)
		$N9_{pyr}$	2.946 (9)
$N8_{ring}$	3.020 (9)	$N12_{ring}$	2.985 (10)
$O11_{ring}$	2.750 (9)	$O15_{ring}$	2.814 (7)
$O14_{ring}$	2.778 (8)	$O18_{ring}$	2.828 (8)
$N17_{ring}$	3.050 (9)	$N21_{ring}$	2.949 (9)
$O20_{ring}$	2.837 (8)	$O24_{ring}$	2.824 (9)
$O23_{ring}$	2.824 (9)	$O27_{ring}$	2.840 (8)
$O32_{ph}$	2.943 (10)	$O38_{ph}$	3.056 (9)
$O36_{DMF}$	2.615 (10)	$N40_{pyr}$	2.982 (9)
$O37_{w}$	2.728 (10)	$O43_{w}$	2.807 (9)

It was possible to locate positions for H4, the hydrogen atom bonded to O4, and the two water hydrogen atoms, H37A and H37B, in difference maps. These three hydrogen atoms are involved in hydrogen bonding with the bromide ions (see Table 5). It was not possible to find a reasonable position for hydrogen H32 in the final difference map, but the presence of two bromide anions in the solid state structure establishes that O32 is protonated. The short interatomic distance between O32 and Br2 suggests that there is a hydrogen bond between them.

In contrast to uncomplexed **10**, the ligand in the Ba^{2+} complex has both lariat arms on the same side of the diaza-18-crown-6 cavity and the CHQ groups have rotated so that their donor atoms point into the cavity of the diazacrown ring. The complex is shown in Figure 8. The large conformational change in **10** during complexation is evident when one compares Figure 6 with Figure 8. In the complex, all 10 donor atoms of **10** are involved in coordination with Ba^{2+}. The eleventh coordination site of Ba^{2+} is occupied by a water molecule. It is apparent in Figure 8 that, in the presence of Ba^{2+}, the complexing ligand **10** resembles a cryptand. This has been discussed previously[6] as a justification for the large log *K* value (see Table 1) for the formation of Ba^{2+}−**10**. The two CHQ groups of this molecule are held rigidly in place as each acts as a bidentate donor. This is in contrast to Ba^{2+}−**9** in which each lariat arm has only one donor atom to complex with the metal ion. It was possible to locate positions for the water hydrogen atoms and also for H7, the hydrogen of one of the CHQ hydroxy groups in the difference map, but it was not possible to locate the other phenol

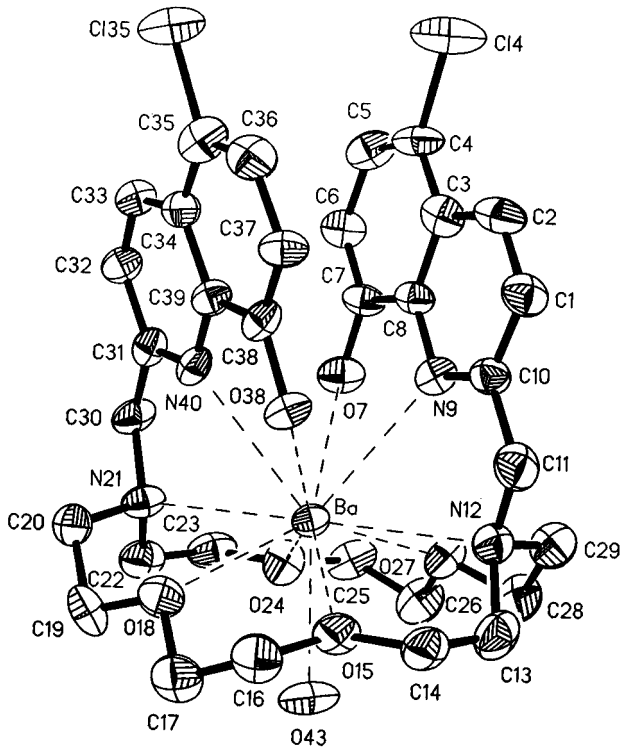

Figure 8. Computer drawing of Ba^{2+}−**10**, including the water ligand. The bromide ions, chloroform molecules, the unidentified molecule, and hydrogen atoms are omitted for clarity. Thermal ellipsoids were drawn at the 40% probability level.

hydrogen atom (H38). Hydrogen atom H7 and the water hydrogens, H43A and H43B, are involved in hydrogen bonds involving the bromide ions in a manner similiar to that found in Ba^{2+}−**9** (see Table 5). It is likely that O38 also interacts with a bromide ion as the O38···Br2 interatomic distance is rather short.

In summary, the Ba^{2+} complexes with **9** and **10** have some similarities but also some significant differences. In both complexes, the phenol hydrogens are not lost during complexation. In both complexes, Ba^{2+} interacts with all of the donor atoms of the diaza-18−crown-6 portion of the respective ligands and also with a water of solvation. Also in the two complexes, the water ligand is involved in hydrogen bonding with the bromide ions. However, there is a significant difference in the role of the lariat arms in the two complexes. In Ba^{2+}−**9**, only one arm is involved in complexation and this group has only one donor atom. By contrast, both arms are positioned over the cavity in Ba^{2+}−**10**, and each CHQ acts as a bidentate ligand. The quinoline groups interact with each other and form a pseudo-cryptand. The Ba^{2+}−donor atom interatomic distances are similar. The average $Ba^{2+}-O_{ring}$ distance in Ba^{2+}−**9** is slightly shorter than the average of similar distances in Ba^{2+}−**10**, while the $Ba^{2+}-N_{ring}$ interatomic distances are longer in Ba^{2+}−**9**. The DMF oxygen−Ba^{2+} distance (2.615 Å) is the shortest of all of the Ba^{2+}−donor atom distances in the two complexes, while the $Ba^{2+}-O_{phenyl}$ distances in Ba^{2+}−**10** are the longest (see Table 6).

Experimental Section

All nuclear magnetic resonance spectra were obtained at 200 MHz in $CDCl_3$. HRMS (CI and low-voltage ionization) was used to record the mass spectra. UV−visible spectra were recorded at 25 ± 1 °C in a 1 cm quartz cell by using an 8452 Å Diode Array spectrophotometer. Solvents and starting materials were used as purchased. Compounds **5**,[8a] **8**,[8b] **12**,[9] and **17**[16] were synthesized as described. Reagent grade inorganic chemicals were obtained from the indicated sources and used without further purification: NaBr (J. T. Baker), KBr (Wasatch), CsCl (Fisher), $Mg(ClO_4)_2$ (Allied), $CaCl_2·2H_2O$ (Spectrum), $SrBr_2$ (Spectrum), $BaBr_2$ (Johnson Matthey), $ZnCl_2$ (Mallinckrodt AR), $CuCl_2$ (Aldrich), and $CoCl_2·6H_2O$ (Fisher). Methanol (Fisher HPLC grade) had a water content of less than 0.05%.

Preparation of 7,16-Bis((5-chloro-8-hydroxy-7-quinolinyl)methyl)-1,4,10,13-tetraoxa-7,16-diazacyclooctadecane (1) (Scheme 1). *N*,*N*′-Bis(methoxymethyl)diaza-18-crown-6 (**5**) (1 g, 2.9 mmol) and 1 g (5.6 mmol) of 5-chloro-8-hydroxyquinoline (CHQ) were refluxed in 30 mL of benzene for 10 h. The hot solution was filtered, and the filtrate was evaporated under reduced pressure. The residue was mixed with 15 mL of a hot mixture of benzene and THF (1:1). Compound **1** crystallized when the solution stood for 24 h to give 1.2 g (67%); mp 140−141 °C. ^{1}H NMR: δ 2.97 (t, J = 5.0 Hz, 8 H), 3.71 (m, 16 H), 4.02 (s, 4 H), 7.35 (s, 2 H), 7.49 (m, 2 H), 8.45 (m, 2 H), 8.91 (m, 2 H). MS, *m*/*e*: 645 (M^+). Anal. Calcd for $C_{32}H_{38}O_6N_4Cl_2$; C, 59.53; H, 5.89. Found: C, 59.80; H, 6.01.

7,19-Bis((5-chloro-8-hydroxy-7-quinolinyl)methyl)-1,4,10,13,16-pentaoxa-7,19-diazacycloheneicosane (2) (Scheme 1). *N*,*N*′-Diaza-21-crown-7 (1.5 g, 5 mmol) was treated with 10 mL of a CH_3OH solution of formaldehyde (0.4 g, 13.3 mmol). After standing overnight at 25 °C, CH_3OH was evaporated under reduced pressure. The residue was dissolved in 30 mL of benzene, and 1.6 g (9 mmol) of CHQ was added to the formed *N*,*N*′- bis(methoxymethyl)diaza-21-crown-7 (**6**). The reaction mixture was refluxed for 10 h. The solution was filtered, and the solvent was evaporated under reduced pressure. The slightly yellow oil residue was purified by column chromatography on silica gel (60−200 mesh) using THF/$C_6H_5CH_3$: 1/1 as eluent. Compound **2** (1.8 g, 54%) was isolated as an oil. ^{1}H NMR: δ 3.01 (t, J = 5.3 Hz, 8 H), 3.74 (m, 20 H), 4.08 (s, 4 H), 7.38 (s, 2 H), 7.50 (m, 2 H), 8.45 (m, 2 H), 8.90 (m, 2 H). Anal. Calcd for $C_{34}H_{42}O_7N_4Cl_2$: C, 59.22; H, 6.10. Found: C, 59.05; H, 6.24.

10,22-Bis((5-chloro-8-hydroxy-7-quinolinyl)methyl)-1,4,7,13,16,19-hexaoxa-10,22-diazacyclotetracosane (3) (Scheme 1). This macrocycle was prepared as above for **2** using diaza-24-crown-8 (1.3 g, 3.7 mmol), formaldehyde (0.32 g, 10.7 mmol), and CHQ (1.1 g, 6 mmol). Macrocycle **3** was obtained as an oil (1.2 g, 45%). ^{1}H NMR: δ 2.93 (t, J = 5.0 Hz, 8 H), 3.66 (m, 24 H), 4.06 (s, 4 H), 7.36 (s, 2 H), 7.48 (m, 2 H), 8.45 (m, 2 H), 8.90 (m, 2 H). Anal. Calcd for $C_{36}H_{46}O_8N_4Cl_2$: C, 58.94; H, 6.28. Found: C, 59.09; H, 6.46.

16-((5-Chloro-8-hydroxy-7-quinolinyl)methyl)-1,4,7,10,13-pentaoxa-16-azacyclooctadecane (4) (Scheme 1). *N*-(Methoxymethyl)monoaza-18-crown-6 (**8**) (1.5 g, 4.9 mmol) and 0.8 g (4.5 mmol) of CHQ were refluxed in 30 mL of benzene for 10 h. The hot benzene solution was filtered, and the filtrate was evaporated. The crude macrocycle was purified by column chromatography on silica gel using THF/$C_6H_5CH_3$: 1/1 as eluent to give 1.2 g (56%) of **4** as an oil. ^{1}H NMR δ 2.94 (t, J = 5.2 Hz, 4 H), 3.69 (m, 20 H), 4.02 (s, 2 H), 7.34 (s, 1 H), 7.48 (m, 1 H), 8.46 (m, 1 H), 8.91 (m, 1 H). MS, *m*/*e*: 455 (M^+). Anal. Calcd for $C_{22}H_{31}N_2O_6Cl$: C, 58.09; H, 6.82. Found: C, 58.27; H, 7.00.

7,16-Bis((5-chloro-2-hydroxybenzyl)-1,4,10,13-tetraoxa-7,16-diazacyclootadecane (9) (Scheme 1). Methoxy derivative **5** (1.8 g, 5.1 mmol) and *p*-chlorophenol (1.32 g, 10.3 mmol) were refluxed in 30 mL of benzene for 18 h. After evaporation of the solvent, the residue was solidified by treatment with ether. Column chromatography of the crude material on silica gel using $CHCl_3/CH_3OH$: 50/1 as eluent gave pure **9** (2.1 g, 77%); mp 111−113 °C. ^{1}H NMR: δ 2.87 (t, J = 5.4 Hz, 8 H), 3.66 (m, 16 H), 3.80 (s, 4 H), 6.74 (d, J = 8.5 Hz, 2 H), 6.96 (m, 2 H), 7.12 (m, 2 H). MS, *m*/*e*: 543 (M^+). Anal. Calcd for $C_{26}H_{36}N_2O_6Cl_2$: C, 57.46; H, 6.63. Found: C, 57.36; H, 6.61.

5-Chloro-8-methoxy-2-(bromomethyl)quinoline (13) (Scheme 2). A solution of 5-chloro-8-methoxyquinaldine (**12**) (14 g, 67.5 mmol) in 130 mL of CCl_4 was refluxed with *N*-bromosuccinimide (NBS) (16 g, 89.9 mmol), in the presence of benzoyl peroxide (0.7 g) for 3 days. The hot solution was filtered. The brown filtrate was evaporated to 80 mL and put in the refrigerator. The resulting crystals were filtered and washed with cold CH_3CN. The solid was dissolved in 50 mL of

(16) Black, D. St. C.; McLean, I. A. *Aust. J. Chem.* **1971**, *24*, 1401.

$CHCl_3$, and the solution was washed twice with saturated aqueous Na_2CO_3 and once with water. The organic phase was dried (Na_2SO_4) and evaporated. The product was recrystallized from a mixture of benzene/hexane: 3/1 to give 7 g (36%) of **13**; mp 147−148 °C. ^{1}H NMR: δ 4.07 (s, 3 H), 4.78 (s, 2 H), 6.97 (d, J = 8.4 Hz, 1 H), 7.51 (d, J = 8.4 Hz, 1 H), 7.72 (d, J = 8.8 Hz, 1 H), 8.52 (d, J = 8.8 Hz, 1 H). Anal. Calcd for $C_{11}H_9ONBrCl$: C, 46.07; H, 3.14. Found: C, 46.18, H, 3.18.

7,16-Bis((5-chloro-8-methoxy-2-quinolinyl)methyl)-1,4,10,13-tetraoxa-7,16-diazacyclooctadecane (14) (Scheme 2). Diaza-18-crown-6 (2 g, 7.6 mmol), **13** (4.4 g, 15.4 mmol), and Na_2CO_3 (2.2 g, 20.8 mmol) were refluxed in 120 mL of CH_3CN for 12 h. The reaction mixture was cooled to room temperature and stirred for 1 h. The complex of the final compound with NaBr and the excess Na_2CO_3 were filtered and washed with CH_3CN. The residue was treated with a mixture of water and chloroform (1:4). The organic layer was separated, washed with water, and dried (Na_2SO_4). After evaporation of $CHCl_3$, the residue was dissolved in 10 mL of ethyl acetate and kept in a refrigerator overnight. The resulting crystals were washed with ethyl acetate to give 3 g (61%) of **14**, mp 124−126 °C. ^{1}H NMR: δ 2.90 (t, J = 5.0 Hz, 8 H), 3.67 (m, 16 H), 4.08 (s, 6 H), 4.11 (s, 4 H), 6.92 (d, J = 8.4 Hz, 2 H), 7.46 (d, J = 8.4 Hz, 2 H), 7.99 (d, J = 8.8 Hz, 2 H), 8.45 (d, J = 8.8 Hz, 2 H). MS, *m*/*e* 673 (M^+). Anal. Calcd for $C_{34}H_{42}O_6N_4Cl_2$; C, 60.62; H, 6.24. Found: C, 60.43; H, 6.30.

16-((5-Chloro-8-methoxy-2-quinolinyl)methyl)-1,4,7,10,13-pentaoxa-16-azacyclooctadecane (15) (Scheme 2). Monoaza-18-crown-6 (2.4 g, 9.1 mmol), **13** (2.6 g, 9.1 mmol), and Na_2CO_3 (2 g, 18.8 mmol) were refluxed in 100 mL of CH_3CN for 12 h. After evaporation of the solvent, the residue was treated with a chloroform−water mixture (4:1). The organic layer was separated, washed with water, and dried (Na_2SO_4). After evaporation, the residue was purified by column chromatography on silica gel with chloroform/THF: 10/1 as eluent. Compound **15** was isolated as an oil (3.2 g, 74%). ^{1}H NMR: δ 2.88 (t, J = 5.1 Hz, 4 H), 3.65 (m, 20 H), 4.07 (s, 3 H), 4.11 (s, 2 H), 6.94 (d, J = 8.4 Hz, 1 H), 7.50 (d, J = 8.4 Hz, 1 H), 8.01 (d, J = 8.8 Hz, 1 H), 8.50 (d, J = 8.8 Hz, 1 H); MS, *m*/*e*: 469 (M^+). Anal. Calcd for $C_{23}H_{33}N_2O_6Cl$: C, 58.85; H, 7.04. Found: C, 58.86; H, 7.11.

7,16-Bis((5-chloro-8-hydroxy-2-quinolinyl)methyl)-1,4,10,13-tetraoxa-7,16-diazacyclooctadecane (10) (Scheme 2). Compound **14** (2.1 g, 3.1 mmol) was stirred with LiCl (1 g, 23.5 mmol) in 15 mL of DMF at 130 °C under argon for 15 h. After cooling, the solvent was evaporated and the residue was treated with three portions of ether (30 mL), acidified to pH = 7, and extracted with a $CHCl_3$−H_2O mixture (4:1). The organic and water phases were separated. The $CHCl_3$ layer was washed with aqueous $NaHCO_3$ and then with water and dried (Na_2SO_4). $CHCl_3$ was evaporated under reduced pressure to give a colored oil which solidified from 10 mL of ethyl acetate at 0 °C. The crystals were recrystallized from ethanol to give 1.0 g (48%) of **10**, mp 85−87 °C. ^{1}H NMR δ 2.98 (t, J = 5.1 Hz, 8 H), 3.69 (m, 16 H), 4.10 (s, 4 H), 7.08 (d, J = 8.4 Hz, 2 H), 7.46 (d, J = 8.4 Hz, 2H), 7.84 (d, J = 8.8 Hz, 2 H), 8.43 (d, J = 8.8 Hz, 2 H). MS, *m*/*e*: 645 (M^+). Anal. Calcd for $C_{32}H_{38}O_6N_4Cl_2$: C, 59.53; H, 5.89. Found: C, 59.70; H, 6.00.

16-((5-Chloro-8-hydroxy-2-quinolinyl)methyl)-1,4,7,10,13-pentaoxa-16-azacyclooctadecane (11) (Scheme 2). Macrocycle **11** was prepared as above for **10** from **15** (2.4 g, 5.1 mmol) and LiCl (1 g, 23.5 mmol). Crude compound **11** was purified by column chromatography on neutral alumina using $C_6H_5CH_3$/THF: 1/2 as eluent to give 1.1 g (47%) as an oil. ^{1}H NMR: δ 2.89 (t, J = 5.3 Hz, 4 H), 3.67 (m, 20 H), 4.08 (s, 2 H), 7.07 (d, J = 8.4 Hz, 1 H), 7.45 (d, J = 8.4 Hz, 1 H), 7.79 (d, J = 8.8 Hz, 1 H), 8.43 (d, J = 8.8 Hz, 1 H). MS, *m*/*e*: 455 (M^+). Anal. Calcd for $C_{22}H_{31}N_2O_6Cl$: C, 58.09; H, 6.82. Found: C, 58.16; H, 7.00.

7,16-Bis((5-chloro-8-methoxy-2-quinolinyl)methyl)-1,4,10,13-tetrathia-7,16-diazacyclooctadecane (16) (Scheme 2). Compounds **13** (6 g, 21 mmol) and **17**, (3.4 g, 10.4 mmol) and Na_2CO_3 (6.6 g, 62.3 mmol) were stirred in 150 mL of CH_3CN under reflux for 12 h. After evaporation of the solvent, the residue was extracted with a $CHCl_3$−H_2O mixture (4:1). The $CHCl_3$ layer was separated, washed with water, dried (Na_2SO_4), and evaporated. The residue was washed with hot ethyl acetate and then with ether to give 5.39 g (69%) of **16**, mp 160−162 °C. ^{1}H NMR: δ 2.81 (m, 24 H), 4.07 (s, 10 H), 6.95 (d, J = 8.4 Hz, 2 H) 7.49 (d, J = 8.4 Hz, 2 H), 7.95 (d, J = 8.8 Hz, 2 H), 8.55 (d, J = 8.8 Hz, 2 H). MS, *m*/*e*: 738 (M^+ + 1). Anal. Calcd for $C_{34}H_{42}S_4O_2N_4Cl_2$: C, 55.36, H, 5.70. Found: C, 55.16, H, 5.87.

Determination of Thermodynamic Values. log K (except protonation constants), ΔH, and $T\Delta S$ values were determined as described earlier[10] in CH_3OH at 25.0 ± 0.1 °C by titration calorimetry using a Tronac Model 450 calorimeter equipped with a 20 mL reaction vessel. The metal ion solutions (0.08−0.12 M) were titrated into quinolinocrown ether solutions ((2−4) × 10^{-3} M) and titrations were carried out to a 2-fold excess of the metal ions. The titration experiments showed that all interactions studied had a 1:1 cation−ligand stoichiometry. Processing the calorimetric data according to a 1:1 interaction model gave satisfactory curve fittings between titrated and calculated heats of reaction. Other interaction models usually presented a large deviation in results. Most thermodynamic parameters for metal ion reactions for which log K > 5.5 were determined by a cation competition technique, wherein a solution containing the ligand and one cation was titrated with a solution of a second cation having a larger log K value than the former one.[17] The method used to process the calorimetric data and to calculate the log K and ΔH values has been described.[18]

Determination of Protonation Constants. The protonation constants of **1, 9**, and **10** were determined by potentiometric titration in CH_3OH at 25 °C. The titrations were carried out at a constant ionic strength of 0.10 M $(CH_3)_4NCl$. Potentials to within ±0.1 mV were measured by using an Orion Model 701A digital ion analyzer in conjuction with an Orion combination electrode. The new electrode was conditioned in 2 M $(CH_3)_4NCl$ solutions stepwise to 100% CH_3OH over a 10 day period, starting with the 2 M salt in 90%:10% H_2O:CH_3OH solution. The CH_3OH was increased by 10% per day, while the H_2O was decreased by 10%. Calculations were performed with the SUPERQUAD program using an IBM computer.

X-ray Structure Determinations. Single crystals suitable for the five X-ray structural studies were prepared. Crystal and intensity data were obtained using a Siemens R3m/V automated diffractometer which utilized Mo Kα radiation (λ = 0.710 73 Å). The lattice parameters and orientation matrix for each compound were obtained using a least-squares procedure involving several carefully centered reflections for each crystal. Both **9** and Ba^{2+}−**9** crystallized in the monoclinic space group $P2_1/c$, which was determined uniquely by the systematic extinctions in the intensity data. The other three compounds crystallized in the triclinic crystal system. The intensity statistics suggested that all three compounds crystallized in the centrosymmetric space group $P\bar{1}$, and the three structures were solved successfully using that space group. A summary of the crystal data and experimental parameters for the five structures are listed in Table 7. Structures of the three ligands, **1, 9**, and **10**, were solved using direct methods. In each case the molecules are located about a center of inversion. There are two molecules of **10** in its unit cell (see Table 7), and thus the structure consists of two crystallographically independent but chemically identical molecules. The structures of the two Ba^{2+} complexes were solved by a combination of direct and heavy atom methods. The unit cells of both complexes contained solvent molecules which were located in the respective difference maps. The asymmetric unit of Ba^{2+}−**9** contains a molecule of DMF and a water molecule. The asymmetric unit of Ba^{2+}−**10** contains two molecules of chloroform, one molecule of water, and an additional molecule which is disordered and is located near a center of symmetry. The additional molecule is not one of the solvents used in the crystallization process and has not been identified.

All five stuctures were refined using a full-matrix, least-squares procedure. Non-hydrogen atoms were refined anisotropically except those of the unidentified molecule found in Ba^{2+}−**10**. The positions of the atoms of this molecule were not refined, while the thermal parameters were refined isotropically. Positions for hydrogen atoms bonded to carbon atoms of the ligands in the five compounds and the chloroform molecules in Ba^{2+}−**10** were calculated on the basis of known stereochemical geometery with the C−H distance fixed at 0.96

(17) Lamb, J. D.; Izatt, R. M.; Swain, C. S.; Christensen, J. J. *J. Am. Chem. Soc.* **1980**, *102*, 475.
(18) Eatough, D. J.; Christensen, J. J.; Izatt, R. M. *Thermochim. Acta* **1972**, *3*, 219.

Table 7. Crystal and Experimental Data[a,b]

	1	**9**	**10**	Ba^{2+}−**9**	Ba^{2+}−**10**
formula	$C_{32}H_{38}N_4O_6Cl_2$	$C_{26}H_{36}N_2O_6Cl_2$	$C_{32}H_{38}N_4O_6Cl_2$	[Ba-**9** $(C_3H_7NO)(H_2O)$]Br_2	[Ba−**10**(H_2O)]· $(CHCl_3)_2$· 0.5DS·Br_2
M_r	645.6	543.5	645.6	931.7	NA
$F(000)$	340	576	680	1856	NA
cryst size, mm	0.11 × 0.16 × 0.50	0.14 × 0.38 × 0.55	0.22 × 0.40 × 0.42	0.20 × 0.32 x0.60	0.24 × 0.26 × 0.40
μ, cm^{-1}	2.59	2.96	2.49	33.83	NA
space group	$P\bar{1}$	$P2_1/c$	$P\bar{1}$	$P2_1/c$	$P\bar{1}$
a, Å	6.241(7)	13.407(3)	8.623(3)	11.664(6)	10.655(4)
b, Å	8.675(11)	13.518(6)	10.750(3)	9.717(5)	11.907(5)
c, Å	14.46(2)	7.651(3)	19.236(4)	33.064(11)	19.789(8)
α, deg	87.30(11)	90	84.22(2)	90	84.74(3)
β, deg	88.15(10)	95.93(2)	77.20(2)	91.06(3)	80.70(3)
γ, deg	89.95(10)	90	69.26(2)	90	81.13(3)
V, $Å^3$	782	1379	1625.5	3747	2442
Z	1	2	2	4	2
temp, °C	20	20	20	20	20
ρx, g/cm^3	1.371	1.309	1.319	1.652	NA
λ, Å	0.710 73	0.710 73	0.710 73	0.710 73	0.710 73
2θ limit	53.0°	50.0°	45.0°	45.0°	41.0°
no. of total data	3564	3566	5229	5368	5299
no. of unique data	3256 (R_{int} = 1.70%)	3180 (R_{int} = 2.11%)	4838 (R_{int} = 2.59%)	4910 (R_{int} = 2.39%)	4951 (R_{int} = 2.09%)
no. of obsd data	1741 ($F > 6.0\ \sigma(F)$)	1663 ($F > 6.0\ \sigma(F)$)	3714 ($F > 3.0\ \sigma(F)$)	3224 ($F > 6.0\ \sigma(F)$)	3611 ($F > 4.0\ \sigma(F)$)
R, R_w	0.098, 0.112	0.0410, 0.0554	0.0407, 0.0554	0.0598, 0.0821	0.0538,0.0690
data/pram. ratio	8.8:1	10.2:1	9.4:1	7.9:1	7.1:1
goodness of fit	1.73	1.26	1.22	1.18	1.14
weights	unit weights	$w^{-1} = \sigma^2(F) + 0.0010F^2$	$w^{-1} = \sigma^2(F) + 0.0011F^2$	$w^{-1} = \sigma^2(F) + 0.0037F^2$	$w^{-1} = \sigma^2(F) + 0.0023F^2$
largest peak Δ map, e $Å^{-3}$	0.78	0.19	0.18	1.99	1.12
largest hole in Δ map, e $Å^{-3}$	−0.41	−0.29	−0.24	−1.94	−1.05

[a] DS represents the disordered solvent molecule. NA indicates data not available because of the presence of an unidentified molecule. [b] Uncertainties in the last significant digits are shown in parentheses. $R = \sum||F_o| - |F_c||/\sum|F_o|$. $R_w = [\sum w(|F_o| - |F_c|)^2/\sum(wF_o)^2]^{1/2}$.

Å. Positions for most of the hydrogen atoms bonded to oxygen atoms in these molecules were located in difference maps. It was possible to locate all hydrogen atoms bonded to oxygen atoms in **1**, **9**, and **10** in their respective difference maps. In the complexes, only one hydroxy hydrogen atom could be found in each complex, H4 in Ba^{2+}−**9** and H7 in Ba^{2+}−**10**. The hydrogen atoms of the water molecule in each structure were also located in difference maps. All hydrogen atoms were allowed to ride on their neighboring heavy atoms during the refinement process. Isotropic U values for these atoms in each structure were assigned and were not refined. Weights based on counting statistics were assigned to the data for all structures with the exception of **1** for which unit weights were used. None of the data sets were corrected for absorption or extinction. Atomic scattering factors were taken from published data.[19] All programs used in the solution, refinement, and display of these structures are included in SHELXTL-PLUS.[20]

Acknowledgment. Financial support of this work by the Department of Energy, Basic Energy Sciences Grant No. DE-FG02-86ER13463, and the Office of Naval Research is appreciated. We thank Professor John H. Mangum for his help with the UV−visible spectral experiments.

Supporting Information Available: Tables listing stucture determination information, positional and thermal parameters for all atoms, and anisotropic thermal parameters for non-hydrogen atoms, and figures showing thermal ellipisoid for each structure, UV−visible spectra for free and complexed **1** and **10**, and partial ^1H NMR spectra of free and complexed **1** and **10** (29 pages). This material is contained in many libraries on microfiche, immediately follows this article in the microfilm version of the journal, and can be ordered from the American Chemical Society; see any current masthead page for ordering information.

IC9610290

(19) *International Tables for X-ray Crystallography*; Ibers, J. A., Hamilton, W. C., Eds.; Kynoch Press: Birmingham, England, 1974; Vol. 4, p 99.

(20) Sheldrick, G. M. *SHELXTL-PLUS*; Siemens Analytical X-ray Instruments, Inc.: Madison, WI, 1990.